Werk

Jahr: 1977
Kollektion: fid.geo
Signatur: 8 Z NAT 2148:44
Digitalisiert: Niedersächsische Staats- und Universitätsbibliothek Göttingen
Werk Id: PPN1015067948_0044
PURL: http://resolver.sub.uni-goettingen.de/purl?PPN1015067948_0044

LOG Id: LOG_0025
LOG Titel: Measurement of Lyman-α extinction and energetic charged particle precipitation during the European winter anomaly campaign 1975 - 76
LOG Typ: article

Übergeordnetes Werk

Werk Id: PPN1015067948
PURL: http://resolver.sub.uni-goettingen.de/purl?PPN1015067948
OPAC: http://opac.sub.uni-goettingen.de/DB=1/PPN?PPN=1015067948

Contact

Niedersächsische Staats- und Universitätsbibliothek Göttingen
Georg-August-Universität Göttingen
Platz der Göttinger Sieben 1
37073 Göttingen
Germany
Email: gdz@sub.uni-goettingen.de

J. Geophys. 44, 99 – 106, 1977

Journal of Geophysics

Measurements of Lyman-α Extinction and Energetic Charged Particle Precipitation during the European Winter Anomaly Campaign 1975–76

E.V. Thrane, B. Grandal, O. Hagen, and F. Ugletveit

Norwegian Defence Research Establishment, P.O. Box 25, Kjeller, Norway

Abstract. The paper deals with two different experiments, both designed to measure mesospheric parameters of importance for the understanding of the winter anomaly in ionospheric absorption. Solar Lyman-α is absorbed in the atmosphere mainly by molecular oxygen, and from measurements of its intensity variation with height, density, pressure and temperature may be derived. The results indicate temperatures significantly above the standard atmosphere values in the height range 70–90 km, during winter anomaly conditions, as measured on two Nike-Apache sounding rockets. The same rockets carried GM tubes and a solid state spectrometer to measure the flux of energetic charged particles penetrating into the mesosphere. The results clearly show that ion production from such particles could not have caused enhanced electron densities during the winter anomaly events studied in this campaign.

Key words: Solar lyman-α – Mesospheric temperature – Energetic charged particles – Ion production – Solid state detector.

1. Introduction

Throughout the years since its discovery many mechanisms have been proposed to explain the winter anomaly in ionospheric absorption. The experiments to be described in this paper were designed to test 2 of the hypotheses put forward, a) that the increase in absorption was associated with changes in the state of the neutral atmosphere and b) that increased ion production from precipitation of energetic particles causes enhanced ionization densities (Mæhlum, 1967).

Measurements of the extinction of solar H-Lyman-α radiation have been a successfull means of deriving neutral gas temperature, density and pressure, (Hall, 1972; Thrane and Johannessen, 1975). The experiment consists of a simple ionization chamber, sensitive to the solar radiation at 121.56 nm. The particle fluxes were measured by Geiger Müller tubes and a solid state telescope recently developed at NDRE (Hagen, 1976).

Both experiments were mounted on the rockets code-named BIV I and BIV II, flown from Arenosillo on January 4th, 1976 at 14:30 UT and January 2lst, 1976 at 14:32 UT, respectively. Both rockets reached an altitude of about 130 km. The experiments were partially successful.

2. The Lyman-α Experiment

2.1. Principle of Method

The experiment is based on the fact that H-Lyman-α radiation at 121.6 nm is a very intense line in the solar spectrum, and that this radiation is absorbed in the atmosphere almost exclusively by molecular oxygen, O_2. Consider radiation of intensity I incident at an angle x upon an atmospheric layer of thickness dh with oxygen density $[O_2]$. Then the radiation absorbed in this layer is

$$dI(h) = I(h)\,\sigma[O_2](h)\,\sec x\,dh \tag{1}$$

where σ is the absorption cross section of the radiation. From this equation the density $[O_2]$ may be derived as a function of height h if σ is known and the relative change of intensity with height is measured

$$[O_2](h) = \frac{1}{I(h)} \frac{dI(h)}{dh} \frac{\cos x}{\sigma}.$$

Assuming that the intensity outside the atmosphere, I_∞, is known, the atmospheric pressure is found by integration which yields:

$$p(h) = -K \frac{\cos x}{\sigma} \ln \frac{I(h)}{I_\infty}$$

where K is a constant if the atmospheric gases are completely mixed and σ is assumed to be constant.

A more complete theory including a variation of intensity as well as absorption as a function of wavelength across the width of the solar H-Lyman α line has been described by Hall (1972).

Finally the temperature may be determined from the equation of state

$$T(h) = \frac{\bar{m}\,g}{k} \frac{p(h)}{[O_2](h)} \cdot \frac{1}{K}$$

where k is Boltzmanns constant, $\bar{m}$ the mean molecular mass and g the acceleration of gravity.

2.2. Experimental Technique

The apparatus of the Lyman-α experiment consisted of four parts. These were the detector set, a linear electrometer, a bias voltage supply and an auto-ranging device.

The detector set consisted of two unity gain vacuum-ultraviolet photoionization chambers manufactured by Artech Corporation. The chambers had a copper housing, a lithium-fluoride window and a tungsten centre electrode and were filled with nitric oxide at a pressure of 20 torr. This combination made the chambers sensitive to radiation between 105.0 nm to 135.0 nm. The quantum efficiencies, estimated by the manufacturer, were about 60% at 121.6 nm.

The chambers were mounted as shown in Figure 1 in order to have each chamber point towards the sun once every spin period.

One of the chambers in the detector set had a protection cap, which was released 64 s after launch at an altitude of about 66 km. Lithium Fluoride is a hygroscopic material, and the cap was designed to protect one of the windows from possible changes in sensitivity due to atmospheric humidity. A comparison of the results from the pair of chambers on one of the rockets showed no detectable sensitivity change.

The linear electrometer had a dynamic range from 10^{-10} A to $3{,}2 \times 10^{-8}$ A. The input impedance was 60 MΩ. Internal calibration was performed each 2,2 s during the flight and each calibration lasted 4 ms. Current measurements were made at a sampling rate of 1116 Hz.

An auto-ranging device followed the electrometer. This divided the output swing from the electrometer into eight equal ranges. Between each range was a small amount of hysteresis. Three bits in the telemetry format were used to monitor the range number. With this device the telemetry resolution was expanded from 8 to nearly 11 bits, giving a total current resolution of about 16,5 pA/bit.

A bias voltage of minus 45 V was supplied by a dry charged battery and was applied to the centre electrode of the detector in order to minimize the effects of photoemission.

The angle between the solar rays and the axis of the ionization chambers was determined by an attitude sensor. This sensor consisted of a light-sensitive transistor housed behind two narrow slits forming an angle of 45 degrees. Every spin period the light-sensitive element was triggered twice and the length of the interval between each triggering was measured by counting the PMC-telemetry bit-frequency (250 kbit).

The accuracy of the attitude sensor was estimated to be better than ±1%.

2.3. Results

In the rocket BIV I both Lyman-α detectors as well as the solar attitude sensor functioned well. However, the rocket developed a large coning, and for this reason the sun was not within the aperture of the sensors during parts of the flight. In BIV II only the Lyman-α detector, which was protected by a

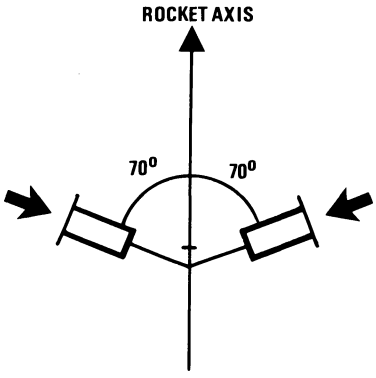

Fig. 1. Orientation of H-Lyman-α detectors

cap, worked and the solar attitude sensor failed. Fortunately this rocket had only moderate coning. The spin rate of both rockets was about 3.5 rps giving about 3 intensity maxima for each detector every second. In order to minimize the effect of noise in the data, the amplitude of each of these maxima was determined by fitting a curve to the data points. Lyman-α intensity as a function of time is shown in Figure 2 for both flights. The intensity corrected for coning is also shown. There is an uncertainty in the determination of I_∞, the intensity outside the atmosphere, and the extreme values possible for this parameter are indicated on the figure. For BIV II the coning correction is based on magnetometer data. The atmospheric pressure, density and temperature were derived from the corrected intensities in the manner outlined in section 2.1.

The uncertainties due to random scatter in the data as well as the effect of systematic errors due to coning and uncertainties in I_∞ were estimated. Figure 3 shows as an example the derived temperatures for BIV II. The derived values are significantly larger than the CIRA (1972) values also indicated in the figure. A detailed discussion of the results will be given elsewhere.

3. The Particle Experiments

3.1. The Particle Detectors

The solid state telescope measured the spectra of precipitating high-energy charged particles. The instrument could resolve electron energies in the range 38 – 800 keV and distinguish between electrons and protons. The instrument had 4 basic parts. These were the sensor unit, the preamplifier, the pulse height analyzer and the bias voltage supply.

The sensor unit was based on 2 silicon surface barrier detectors manufactured by Ortec Corporation, mounted in a telescopic configuration. The front detector was of the totally depleted type with an active area of 50 mm^2 and a thickness of 150 microns. The detector was penetrated by incident electrons with energies >185 keV and protons with energies >4 MeV. The rear detector, which had an active area of 150 mm^2 and a thickness of 1000 microns, was partially

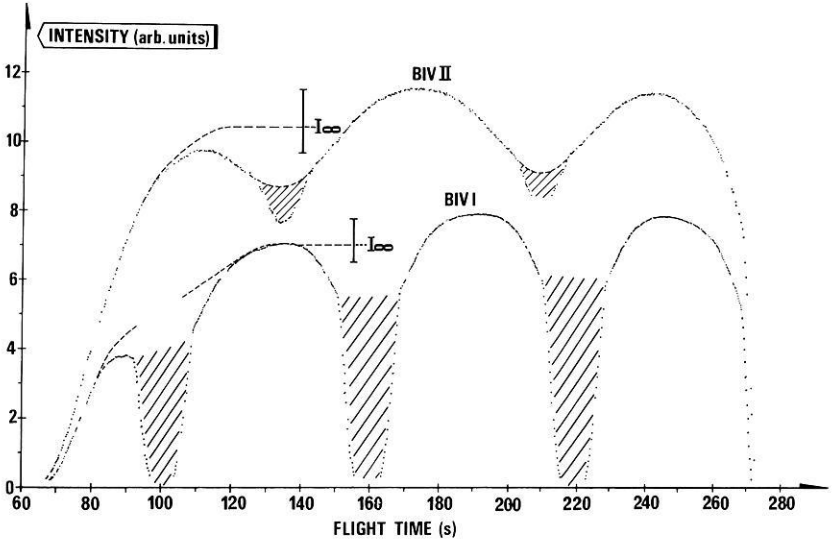

Fig. 2. H-Lyman-α intensity vs. time of flight. *BIV I*: Lower curve. *BIV II*: Upper curve. The hatched regions refer to time intervals when a shadow effect decreased the observed intenstiy

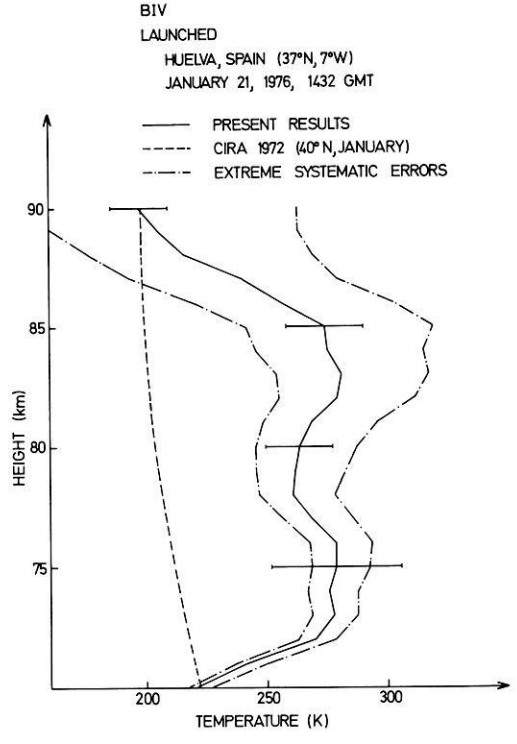

Fig. 3. Temperature vs. height. The temperature profiles are obtained using the different values of I_∞ from figure 2: —— Mean value of I_∞; -·- Extreme values of I_∞

depleted. This detector could resolve electron energies up to 800 keV and measure the integral flux of electrons with higher energies. The relation between the incident electron energy and the energy deposited in the rear detector was for incident electrons >0.25 MeV, according to Katz and Penfold (1952):

$$E_0 = \left(E_1^{1,265} + \frac{\emptyset}{412}\right)^{0,79}$$

where E_0 is the energy of the incident electron in MeV, E_1 is the remaining energy of the electron after penetration of the first detector in MeV and ϕ is the total density of the front detector in mg/cm^2.

The telescope housing and collimator were made of aluminium and polyethylene. Several traps in the collimator served to avoid reflection of particles into the detector. The aluminium side of the front detector pointed outwards to make the telescope insensitive to light.

The geometric factor for the telescope was

$G = 0{,}14$ cm^2 sr.

The preamplifier was of the charge sensitive type. The principle of detection was based on the traditional voltage mode system, where the signal is integrated at the detector to a pulse having a short rise-time followed by a long "tail". The signal was differentiated twice in the two last stages of the amplifier. The sensitivity of the charge sensitive part of the preamplifier was 34 mV/MeV and the resolution was 4.8 keV (fwhm, Si) at zero input capacitance with a noise slope of 64 eV/pF.

The pulse-height analyzer was made of comparators and CMoslogic. The analyzer had eight outputs corresponding to the different energy ranges as shown in Table 1.

The telescope was calibrated by using radioactive sources and an Ortec precision pulse generator, to within an accuracy of 10%.

The bias voltage supply consisted of dry charged batteries embedded in epoxy. The voltage was controlled on – off by a relay and applied to the detectors through an integrating network with a time constant of approximately 2.2 s.

As a supplement to the solid state telescope, two Geiger-Müller counters were flown. The detectors were manufactured by LND, Inc, and were of the type 710. A twelve micron thick mylar sheet was added to one of the detector windows to raise the 50% transmission point (cut-off) from 40 keV to 60 keV. Both detectors were integral counters.

Table 1. Calibration table. All energies in keV

Output		1	2	3	4	5	6	7	8
BIV I	e^-	44–100	100–∞		210–300	300–400	400–550	550–800	800–∞
	p	44–100	100–230	230–4000					4600–∞
BIV II	e^-	38–100	100–∞		220–300	300–400	400–550	550–800	800–∞
	p	38–100	100–230	230–4000					4600–∞

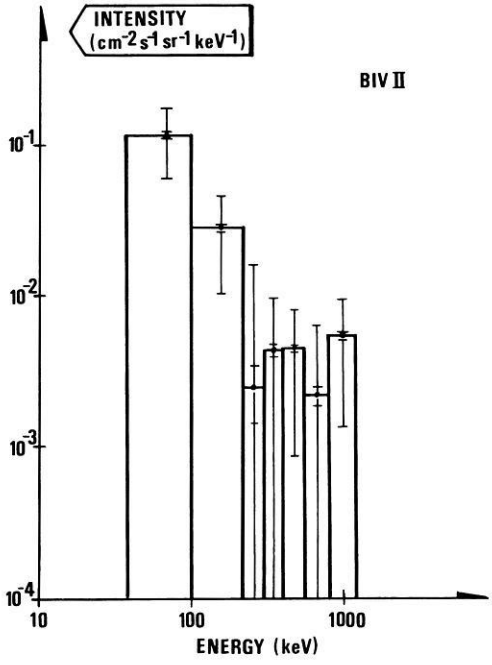

Fig. 4. Differential electron energy spectrum. The error bars indicate the standard deviation and the standard deviation of the mean

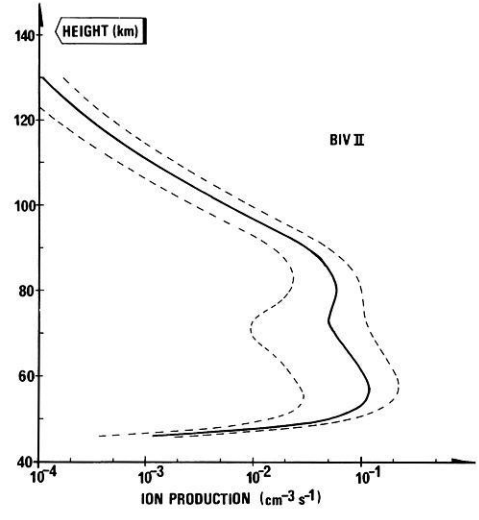

Fig. 5. Ion production vs. height. The dashed curves are obtained using the maximum and minimum values of the error bars in Figure 4

The signal was picked up across a resistor on the groundside of the detector and shaped in a simple network to be compatible to the telemetry. The plateau voltage was supplied from a zener regulated DC-DC converter.

Geometric factors were for both detectors

$G = 3{,}24 \times 10^{-2}\ \mathrm{cm}^2\ \mathrm{sr}.$

3.2. Measurements

In rocket BIV I the door in front of the particle detector assembly failed to open during flight. In rocket BIV II the experiment worked satisfactorially, recording electron and proton precipitation for energies above 38 keV. The particle fluxes were very small, nevertheless a differential energy spectrum shown in Figure 4, was derived from the measurements. This spectrum was used to calculate the ion production as a function of height, (Fig. 5), using the method of Rees (1963). The ion production is very small, much too small to make a significant contribution to the total ion production from normal solar radiation at heights above 70 km. Below 70 km the production is of the same magnitude as the production to be expected from galactic cosmic rays.

4. Conclusions

The two experiments outlined in this paper gave information about the state of the lower ionosphere during winter anomaly conditions. Two tentative conclusions may be drawn from the data. a) The neutral gas temperature in the height range 70–90 km was significantly higher than expected from the standard atmosphere (Cira, 1972). b) The ion production due to precipitating energetic electrons and protons was too small to give a significant contribution to the total ion production, except perhaps between 60 and 70 km.

References

Carver, J.H., Gies, H.P., Hobbs, T.I., Lewis, B.R., McCoy, D.G.. Temperature dependence of the molecular oxygen photo-absorption cross section near the H Lyman-α line. J. Geophys. Res. **72**, 1955, 1977

Cospar International Reference Atmosphere, Berlin: Akademie-Verlag 1972

Hagen, O.: A solid state telescope for measuring energy spectra of precipitating charged particles in sounding rockets. Technical Note E-805, Norwegian Defence Research Establishment 1976

Hall, J.E. Atmospheric pressure, density and scale height calculated from H-Lyman-α absorption allowing for the variation of cross section with wavelength. J. Atmos. Terr. Phys. **34**, 1337, 1972

Katz, L., Penford, A.S.: Range-energy relations for electrons and the determination of beta-ray end-point energies by absorption. Rev. Mod. Phys. **24**, 28, 1952

Mæhlum, B.N.: On the "Winter Anomaly" in the midlatitude D-region. J. Geophys. Res. **72**, 2287, 1967

Rees, M.H.: Auroral ionization and excitation by incident energetic electrons. Planet. Space Sci. **11**, 1209, 1963

Thrane, E.V., Johannessen, A.: A measurement of the extinction of solar hydrogen Lyman-α radiation in the arctic mesosphere. **37**, 655, 1975

Received May 2, 1977

Note Added in Proof

New values of the photo absorption cross section of molecular oxygen near the Lyman-α line have been used to derive the results in Figure 3 (Carver et al., 1977)